HHS Public Access

Author manuscript

Biol Psychiatry Cogn Neurosci Neuroimaging. Author manuscript; available in PMC 2019 January 01.

Published in final edited form as:

Biol Psychiatry Cogn Neurosci Neuroimaging. 2018 January ; 3(1): 50–58. doi:10.1016/j.bpsc.2017.07.001.

EEG source functional connectivity reveals abnormal high-frequency communication among large-scale functional networks in depression

Alexis E. Whitton[1,2], **Stephanie Deccy**[1], **Manon L. Ironside**[1], **Poornima Kumar**[1,2], **Miranda Beltzer**[1], and **Diego A. Pizzagalli**[1,2]

[1]Center for Depression, Anxiety and Stress Research, McLean Hospital, Belmont, MA, USA

[2]Department of Psychiatry, Harvard Medical School, Boston, MA, USA

Abstract

Background—Functional magnetic resonance imaging studies of resting-state functional connectivity have shown that major depressive disorder (MDD) is characterized by increased connectivity within the default mode network (DMN) and between the DMN and the fronto-parietal network (FPN). However, much remains unknown about abnormalities in higher frequency (>1 Hz) synchronization. Findings of abnormal synchronization in specific frequencies would contribute to a better understanding of the potential neurophysiological origins of disrupted functional connectivity in MDD.

Method—We used the high temporal resolution of electroencephalography (EEG) to compare the spectral properties of resting-state functional connectivity in individuals with MDD (n=65) to healthy controls (n=79), and examined the extent to which connectivity disturbances were evident in a third sample of individuals in remission from depression (rMDD; n=30). Exact Low Resolution Electromagnetic Tomography (eLORETA) was used to compute intra-cortical activity from regions within the DMN and FPN, and functional connectivity was computed using lagged phase synchronization.

Results—Compared to controls, the MDD group showed greater within-DMN beta-2 band (18.5–21 Hz) connectivity and greater beta-1 band (12.5–18 Hz) connectivity between the DMN and FPN. This hyperconnectivity was not observed in the rMDD group. However, greater beta-1 band DMN-FPN connectivity was associated with more frequent depressive episodes since first depression onset, even after controlling for current symptom severity.

Corresponding Author: Diego A. Pizzagalli, Center for Depression, Anxiety and Stress Research, McLean Hospital, 115 Mill Street, Belmont, MA USA 02478, Phone: +1 (617) 855-4230, Fax: +1 (617) 855-4231, dap@mclean.harvard.edu.

Financial Disclosures: Over the past three years, Dr. Pizzagalli has received consulting fees from Akili Interactive Labs, BlackThorn Therapeutics, Boehringer Ingelheim, Pfizer and Posit Science, for activities unrelated to the current project. All other authors report no biomedical financial interests or potential conflicts of interest.

Conclusions—These findings extend our understanding of the neurophysiological basis of abnormal resting-state functional connectivity in MDD and indicate that elevations in high-frequency DMN-FPN connectivity may be a neural marker linked to a more recurrent illness course.

Keywords

major depression; resting-state functional connectivity; eLORETA; lagged phase synchronization; default mode network; fronto-parietal network

Introduction

Major depressive disorder (MDD) is a heterogeneous condition characterized by deficits in emotional, cognitive and motor functioning. Commensurate with its symptomatic complexity, recent conceptualizations view MDD as a systems-level disorder that arises from dysregulation among large-scale functional brain networks [1–4]. Connectivity among these networks has been commonly probed by examining the correlation in blood oxygen level-dependent (BOLD) fluctuations between brain regions under task-free conditions using functional magnetic resonance imaging (fMRI). However, since this is limited to the speed of the hemodynamic response, fMRI-based connectivity is restricted to frequencies below 1 Hz, and it is unclear whether higher frequency neuronal synchronization contributes to connectivity disturbances in depression. This is important because it has been posited that each functional network may be characterized by a unique electrophysiological signature [5, 6], and the spectral specificity of this electrophysiological signature may represent a way in which the brain builds a hierarchical structure of interconnected networks [7]. Accordingly, differences in the spectral properties of resting-state networks in depression may point to differences in the hierarchical organization of these networks, which may underpin differences in the cross-talk between networks.

Functional networks are spatially distributed sets of brain regions that exhibit temporally correlated activity. Studies have shown that these networks are evident even in the brain's intrinsic activity during the resting state, termed resting-state functional connectivity [rsFC; 8, 9]. fMRI studies have consistently observed disruptions in the default mode network (DMN) and the fronto-parietal network (FPN) in individuals with depression [4]. The DMN is comprised of regions that exhibit greater activity under task-free conditions relative to conditions requiring goal-directed behavior [10] and include the medial prefrontal cortex, the posterior cingulate cortex and precuneus, as well as bilateral inferior temporo-parietal cortexes and medial temporal lobes [11]. This network is thought to subserve self-referential processing, memory and the allocation of attentional resources for cognitive processing [11]. In contrast, the FPN includes a set of brain regions involved in the top-down modulation of attention and emotion and includes portions of the lateral prefrontal cortex and posterior parietal cortex. The FPN is implicated in cognitive control [12], and inhibits the DMN when it is irrelevant to task performance [13]. In the context of depression, evidence suggests that abnormal within-DMN rsFC may underlie the tendency for depressed individuals to engage in negative self-referential thought [14], whereas abnormalities in within-FPN rsFC may underpin depression-related cognitive deficits [15]. Furthermore, a failure of the FPN to

effectively inhibit DMN activity may result in problems shifting attention away from internal thoughts to the external world and is one mechanism that may drive rumination [4, 16].

Electroencephalography (EEG) provides a direct measure of postsynaptic potentials with millisecond temporal resolution, and a means of studying the high temporal dynamics of functional networks. Approaches to estimating functional connectivity in EEG at the sensor level have been confounded by the diffusion of the EEG signal by the skull, however advances in source localization [17] have made it possible to minimize these confounds. Although the field is still in its infancy, several groups have begun to examine rsFC using measures of lagged connectivity between EEG source estimates. In applying this method, exact Low Resolution Electromagnetic Tomography [eLORETA; 17] – a linear inverse solution – is first used to compute the distribution of current density across voxels in the brain. Next, connectivity between intra-cortical sources is computed using lagged phase synchronization. This measure corrects for the effects of volume conduction as it represents the connectivity of two signals after the potentially artifactual zero-lag contribution has been excluded. Importantly, it can be applied to filtered data, allowing for the decomposition of connectivity at individual frequencies.

Findings emerging from studies using this method highlight its promise as a tool for probing the spectral properties of rsFC disturbances. Research has revealed rsFC disturbances within discrete frequency bands in Alzheimer's Disease [18, 19], psychosis [20–22], obsessive-compulsive disorder [23], post-traumatic stress disorder [24] and eating disorders [25]. To date, only one study has used lagged phase synchronization to examine the spectral properties of connectivity disturbances in MDD [26]. This study focused on connectivity between a targeted set of frontal brain regions previously associated with metabolic or anatomical abnormalities in MDD. Individuals with MDD had increased alpha-band lagged phase synchronization between the subgenual anterior cingulate cortex and both the left medial prefrontal cortex and left dorsolateral prefrontal cortex [26]. However, these findings are difficult to interpret in the context of an association between increased alpha-band lagged phase synchronization and *greater* symptom improvement after antidepressant treatment. Furthermore, it remains unknown to what extent altered high-frequency rsFC might represent a state or trait-like marker of MDD.

Therefore, we aimed to capitalize on the high temporal resolution of EEG to investigate the spectral dynamics of rsFC across different frequencies in the DMN and FPN in individuals with MDD. As prior fMRI studies have shown increased within-network connectivity in the DMN and decreased within-network connectivity in the FPN in depression [16], we predicted that relative to healthy controls, individuals with MDD would exhibit stronger rsFC among regions of the DMN and weaker rsFC among regions of the FPN. Furthermore, given that deficits in emotion regulation in depression are postulated to result from a failure of fronto-parietal control systems to regulate DMN activity (indicated by less anticorrelated activity between these networks [4]), we also predicted that individuals with MDD would exhibit stronger between-network rsFC between regions of the DMN and FPN. In light of evidence suggesting that communication among resting-state networks may be driven by synchronization in discrete frequency bands, a critical aim was to determine whether any

connectivity abnormalities observed those with MDD were restricted to certain frequency bands. Finally, we compared rsFC in individuals with MDD to an independent sample of individuals in remission from depression (rMDD) to examine the extent to which high-frequency connectivity abnormalities might represent a trait-like vulnerability marker for the condition.

Method

Participants

Seventy-nine healthy control participants and 65 individuals with MDD were recruited from the greater Boston area. Additionally, data from a smaller subsample of 30 individuals with rMDD were used in secondary analyses. All participants were right-handed, aged 18–65, had no history of neurological conditions, head injury, or seizures, and were free from recreational substances as indicated by a negative urine drug screen on the day of testing (Amedicheck CLIA-Waved 12-panel cup; Branan Medical Corporation, Irvine, California). Control participants were eligible if they had no lifetime DSM-IV diagnoses, no first-degree relatives with psychiatric illnesses, had a Beck Depression Inventory-II [BDI-II; 27] score < 13 and no lifetime use of psychotropic medication. MDD participants were eligible if they had a current MDD diagnosis according to the Structured Clinical Interview for DSM-IV [SCID-IV; 28], had been on stable antidepressant medication over the past 8 weeks or had taken no psychotropic medication for at least 2 weeks (drug-specific washout periods were applied), and had MDD as their primary diagnosis. rMDD subjects were required to have had at least one major depressive episode (MDE) in the past 5 years, had been in remission for at least 8 weeks as indicated by a score of 1 on the Depressed Mood and Anhedonia items from the SCID-IV, and were free of psychotropic medication (wash-out periods were applied). Certain past comorbidities were allowed if in remission at the time of testing and secondary to the MDD (see Supplement). All participants provided written informed consent.

Procedure

Prior to EEG, subjects were administered the SCID-IV by Masters-level or PhD-level clinical interviewers. Those deemed eligible took part in a resting EEG recording on the same day as their SCID assessment, or shortly thereafter. At their EEG recording, participants completed the BDI-II to assess depressive symptom severity. They also completed the Mood and Anxiety Symptom Questionnaire [MASQ; 29], which yields four subscores: General Distress Anxious Symptoms (GDA), General Distress Depressive Symptoms (GDD), Anxious Arousal (AA), and Anhedonic Depression (AD). In the current sample, the BDI-II (α=0.97), total MASQ (α=0.86), and MASQ subscales (GDA α=0.91; GDD α=0.98; AA α=0.90; AD α=0.75) had good internal consistency.

EEG recording and data reduction

EEG was recorded using a 128-channel Hydrocel Geodesic Sensor Net system (Electrical Geodesics, Inc., Eugene, Oregon), sampled at 250 Hz (bandwidth 0.1–100 Hz; impedances < 100 kΩ), referenced online to Cz. Data were acquired in eight 1-minute segments (four eyes open, four eyes closed), which were randomized and counterbalanced across

participants. Consistent with prior EEG research on depression [30], only eyes closed data were analyzed. Data processing occurred offline using BrainVision Analyzer 2.0 (Brain Products GmbH, Gilching, Germany). First, muscle artifacts were manually removed, then blinks and electrocardiogram were removed using independent components analysis [31]. Due to the influence of ICA correction on coherence measures [32], only ICA components without visible neural activity were removed. Corrupted channels were interpolated using a spline interpolation [33]. The EEG was then visually inspected, remaining artifacts removed, and re-referenced to the average reference. After processing, non-overlapping 2.048 s segments were extracted for connectivity analyses. As recommended by Pascual-Marqui et al. [17], all participants had a minimum of 40 s of artifact-free data available for analysis.

Regions of interest (ROIs)

Seeds from key regions within the DMN and FPN were selected from the seven-network parcellation described in Yeo et al. [34], and then used to create ROIs in eLORETA. Given the lower spatial resolution of eLORETA (voxel dimension: 5 mm^3), bilateral seeds close to the midline were fused into a single seed, and subcortical seeds omitted. ROIs were created by including all gray matter voxels within a 10 mm radius of the seed. There were ten ROIs from the DMN and nine from the FPN. The Montreal Neurological Institute (MNI) coordinates for the seeds are listed in Table 1.

Source-based functional connectivity

We computed EEG source-based functional connectivity using eLORETA software [17]. eLORETA is a linear inverse solution that can reconstruct cortical activity with correct localization from scalp EEG data [17]. The solution space consists of 6239 cortical gray matter voxels in a realistic head model [35] using the MNI152 template [36]. The LORETA algorithm (upon which eLORETA is based) has been validated in several studies combining LORETA with fMRI [37–39], PET [40, 41], simultaneous EEG-fMRI [42, 43] and intracranial recordings [44].

Lagged phase synchronization, a measure that quantifies the non-linear relationship between two regions after removal of the instantaneous contribution, was then computed across DMN and FPN ROIs. Instantaneous measures of EEG-based connectivity are known to be susceptible to the effects of volume conduction, which can lead to the detection of spurious functional coupling among separate regions. However, lagged connectivity corrects for this as it represents the connectivity between two regions after this zero-lag contribution has been excluded. In this respect, lagged connectivity is considered to represent a true measure of physiological connectivity. Lagged phase synchronization between ROIs was computed for each artifact-free EEG segment in the frequency domain using normalized Fourier transforms. Based on prior factor analyses of distinct frequency bands [45], the frequency ranges were: delta (1.5–6 Hz), theta (6.5–8 Hz), alpha-1 (8.5–10 Hz), alpha-2 (10.5–12 Hz), beta-1 (12.5–18 Hz), beta-2 (18.5–21 Hz) and beta-3 (21.5–30 Hz). For additional details see Supplement.

Functional connectivity analyses

Group differences in within- and between-network connectivity were examined by comparing lagged phase synchronization between all pairs of ROIs in the DMN and FPN at each frequency simultaneously. Analyses were first conducted using *t*-tests that were corrected for multiple comparisons using a non-parametric permutation procedure (5000 randomizations; see Supplement for additional details). To further probe group differences in connectivity, this was followed up using a less conservative approach where *t* values were thresholded at $p<0.001$ (uncorrected).

Secondary analyses

For connections showing significant group differences, we performed a one-way ANOVA to evaluate whether any connectivity abnormalities in those with acute MDD were also evident in individuals in remission. Furthermore, we examined correlations between these connectivity indices and depression severity and illness course. Finally, at the suggestion of a reviewer, follow-up analyses were conducted to determine the extent to which putative group differences generalized to within-DMN and DMN-FPN connectivity more broadly by comparing the MDD and HC groups in their mean connectivity of all within-network or between-network pairs. Results from these analyses were generally consistent with those reported in the main text and are presented in full in the Supplement.

Results

Sample characteristics

Demographic and clinical characteristics are summarized in Table 2. The groups did not differ as a function of sex or education (all ps>0.05). Although the HC and MDD group did not differ in terms of age, the rMDD group was older than the HC group ($p=0.04$). The MDD group scored higher than the HC and rMDD groups on the BDI-II and the four MASQ subscales (all ps<0.001), and had more lifetime comorbidities compared to the rMDD group ($p=0.006$). Ten subjects in the MDD group were medicated (see Supplement). Within the MDD group, demographic and clinical characteristics did not differ as a function of medication status (all ps>0.05).

Effects of acute depression on within-network connectivity

Significant differences between the HC and MDD groups emerged for within-DMN connectivity (Fig. 1A). The MDD group had stronger lagged phase synchronization between a region in the right superior frontal gyrus (SFG; corresponds to region ‘R DMN-A’ in Table 1) and a region in the right parahippocampal gyrus (PHG; region ‘R DMN-E’ in Table 1), in the beta-2 frequency band (18.5–21 Hz; $p<0.05$, FWE-corrected). Contrary to our hypotheses, there were no group differences in within-FPN connectivity when examined at $p<0.05$ FWE-corrected or $p<0.001$ (uncorrected).

Effects of acute depression on between-network connectivity

The HC and MDD groups also differed with respect to between-network connectivity (Fig. 1B). Specifically, the MDD group showed stronger lagged phase synchronization between a

region in the left SFG (region 'L DMN-A' in Table 1) and a region in the right middle temporal gyrus (MTG; region 'R FPN-C' in Table 1) in the beta-1 band (12.5–18 Hz; $p<0.001$ uncorrected). Supplementary Fig. 1 shows maps of connectivity differences between the MDD and HC groups.

Connectivity following depression remission

To determine whether these abnormalities may be a trait-like marker that persists beyond symptom remission, we compared the indices of beta-2 within-DMN connectivity, and beta-1 DMN-FPN connectivity in the MDD and HC groups to an independent sample of rMDD individuals.

A one-way ANOVA revealed a main effect of *Group* (HC, MDD, rMDD) for within-DMN beta-2 connectivity between the right SFG and right PHG, $F(2,171)=10.01$, $p<0.001$, $\eta_p^2=0.10$. Bonferroni-corrected pairwise comparisons showed DMN connectivity was higher in the MDD group relative to both the HC ($p<0.001$, Cohen's $d=0.73$) and rMDD groups ($p=0.03$, $d=0.59$), but did not differ between the rMDD and HC groups ($p=1.00$, $d=0.16$).

The same pattern emerged for between-network beta-1 connectivity between the left SFG and right MTG. Specifically, the main effect of *Group* was significant, $F(2,171)=9.74$, $p<0.001$, $\eta_p^2=0.10$, and post-hoc tests showed DMN-FPN connectivity was again higher in the MDD group compared to the HC ($p<0.001$, $d=0.68$) and rMDD groups ($p=0.008$, $d=0.66$), but the rMDD and HC groups did not differ ($p=1.00$, $d=0.03$). These findings did not change when controlling for age (all ps<0.05), which was higher in the rMDD compared to the HC group. Findings also remained unchanged when medication status was entered as a covariate (all ps<0.05).

Associations between connectivity disturbances and depressive illness severity

When examining the MDD group separately, Spearman's rank order correlations did not reveal any significant associations between current depressive symptom severity on the BDI or MASQ GDD subscale, and either enhanced within-network DMN connectivity, or enhanced between-network DMN-FPN connectivity (all ps>0.05).

Additional correlations were conducted to examine associations between connectivity disturbances and illness severity in the MDD and rMDD groups. Forty-three MDD subjects and 27 rMDD subjects had information available on their self-reported age of first depression onset and the number of MDEs experienced in their lifetime (Table 2). The groups did not differ in age of onset, $t(68)=1.19$, $p=0.24$, $d=0.28$, however the MDD group reported more lifetime MDEs, $t(68)=2.16$, $p=0.03$, $d=0.58$.

In line with prior research [e.g., 46], a measure of depressive illness severity was computed as the ratio of lifetime MDEs to the number of years since first depression onset, as a gauge of episode frequency. After computing this, three subjects were excluded from further analyses for having a depressive illness severity score > 3SDs from the mean. Correlations showed greater depressive illness severity was associated with greater beta-1 DMN-FPN connectivity (Spearman's rank correlation $rho=0.32$, $p=0.01$, $N=67$; Fig. 2). This association

remained significant when controlling for current depression severity on the MASQ GDD subscale (partial *rho*=0.29, *p*=0.02). This indicates that, whereas connectivity disturbances normalized in remitted individuals, for those with a history of depression, a more severe depressive illness course was associated with stronger high-frequency DMN-FPN connectivity.

Discussion

Our findings revealed abnormally elevated lagged phase synchronization within the DMN and between regions of the DMN and FPN in individuals with MDD, which emerged in the beta-band. Although these connectivity disturbances were not evident in those with rMDD (indicating some normalization following remission), variability in lifetime MDE frequency correlated with between-network connectivity across MDD and rMDD groups. Specifically, enhanced DMN-FPN beta-band connectivity was associated with more frequent MDEs since first depression onset, and may therefore be a marker of a more recurrent depressive illness course.

These findings are consistent with those of fMRI studies examining rsFC disturbances in MDD. For example, we observed enhanced phase synchronization between the right SFG and right PHG (regions in the DMN) in the MDD group. These regions overlap with those of a recent fMRI-based meta-analysis, which showed evidence of hyperconnectivity between DMN regions and regions of the hippocampus in those with MDD [4]. The PHG is thought to be the primary node in the medial temporal DMN subsystem that mediates connectivity between DMN regions and structures such as the hippocampus that support autobiographical recall [47]. Connectivity between the PHG and other DMN regions has been found to become enhanced in depressed individuals during recall of negative events [48]. This has also been observed in individuals with rMDD [49], and linked with greater severity of ruminative thoughts, supporting a role for enhanced within-DMN connectivity in rumination. Our observation of enhanced DMN-FPN between-network synchronization in the MDD group, involving the left SFG (DMN) and the right MTG (FPN), also aligns with evidence of enhanced correlation in BOLD signal between the right MTG and DMN regions (including the left SFG) in depression, which were purported to arise from gray matter abnormalities in the right MTG [50]. According to a meta-analysis of fMRI rsFC studies [4] and a recent review on rsFC abnormalities in psychopathology [51], enhanced DMN-FPN connectivity may reflect either a weakness of the FPN to modulate the DMN, or the DMN “enslaving” the FPN. Whatever the mechanism, this hyperconnectivity between networks is hypothesized to underpin impairments in goal-directed behavior and a cognitive style that is biased toward internal (often negative), self-referential thoughts.

The convergence of findings across modalities is encouraging; however, a critical question is whether knowledge of the spectral properties of these disturbances tells us something new about MDD pathophysiology. We showed that elevations in phase synchronization within and between networks in the MDD group emerged in the beta-band (12.5–21 Hz). The precise processes that beta-band oscillations support remains a topic of debate, however, one view is that beta synchronization promotes the maintenance of a current motor or cognitive state, and is increased in contexts where the brain’s ‘status quo’ is given priority over new

signals [52, 53]. Support for this theory comes from studies showing that pathological enhancement of beta-band synchronization can lead to deterioration of flexible motor and cognitive control. For example, elevated cortico-basal ganglia beta-band synchronization has been linked to impairments in initiating voluntary movement in Parkinson's Disease [54–56] and artificially inducing excessive beta synchronization via intracranial electrical stimulation of the basal ganglia causes the emergence of movement symptoms [57]. In light of its predominance at rest, beta-band synchronization has been suggested to correspond to an 'idling rhythm' in the motor system [58].

Similarities appear in regard to cognitive functioning and suggest beta-band synchronization may also correspond to a cognitive idling rhythm. Non-human primate studies have shown that synchronization in the beta-band is strongest during tasks requiring a high degree of endogenously-driven attention and lowest on tasks requiring processing of novel or unexpected external events [59, 60]. Engel and Fries [52] suggest that strong beta-band synchronization across a neuronal population promotes the maintenance of a motor or cognitive state because the signal of this neuronal assembly overrides any signals coming from new inputs. Building on this, they suggest that the DMN should be distinguished by prominent beta-band synchronization, since it constitutes a state characterized by low expectation of change. Indeed, several studies have revealed positive associations between absolute beta-band power and BOLD signal change in the DMN [5, 61–63]. In the context of our findings, the elevated beta-band synchronization involving DMN regions in the MDD group may reflect highly synchronized neuronal populations, the signal from which is processed at the expense of other inputs that signal the need to flexibly modulate the DMN in accordance with changing cognitive states. This theory is of course speculative, and future studies (e.g., using neuromodulation techniques to entrain beta oscillations) are needed to directly test whether excessive beta-band synchronization contributes to DMN inflexibility.

These findings demonstrate one of the ways in which studying the spectral properties of connectivity disturbances may provide insight into the neurophysiological origin of network abnormalities in psychopathology, and there are several important avenues for future research. In this study, we conceptualized functional connectivity as a static process involving patterns of phase synchronization that are stable across the recording period. However, an emerging field is 'dynamic' functional connectivity [64], which refers to the variability in the strength or spatial organization of connectivity among networks over time. Recent fMRI research shows that in depression, persistent internally focused attention may be linked to decreased variability in connectivity within the DMN (driven by a more persistent positive correlation in activity among regions in the DMN over time), along with increased variability in connectivity between the DMN and regions implicated in regulating attention [65]. EEG-based connectivity measures may provide two important extensions to this work: (1) they can reveal how the strength, spatial organization and *spectral properties* of connectivity among brain systems converge and diverge over time, and (2) they can capture these changes on a millisecond timescale. If beta-band synchronization is implicated in maintaining cognitive states (particularly the default mode), then one might expect that excessive beta-band connectivity would be associated with reductions in dynamic functional connectivity in the DMN.

Some limitations must be kept in mind when interpreting our findings. Several key brain regions implicated in MDD pathophysiology are subcortical, and since eLORETA can only reliably estimate activity in cortical regions, we could not examine connectivity in these regions. In addition, although we observed abnormal rsFC in the beta-band in MDD, neural networks likely involve coordinated communication across frequencies [66] and an obvious extension of our work is to examine measures of lagged cross-frequency coupling. Finally, although we used several pre-requisite parameters for conducting functional connectivity on EEG source estimates, such as using a high-density EEG montage and a realistic head model [67, 68], due to the limitations and inherently low spatial resolution of eLORETA, we cannot rule out that synchrony between ROIs may be related to activity from regions adjacent to the ROIs. As such, our findings await replication using methods that have superior spatial resolution.

In sum, we show that depression is characterized by elevated within-DMN and DMN-FPN phase synchronization in the beta-band, which normalizes to some extent following symptom remission but is associated with a more recurrent depressive illness course. Excessive beta-band synchronization, which has been associated with maintaining the brain's 'status quo', may be a mechanism that drives DMN inflexibility in depressed individuals. These findings highlight measures of EEG source functional connectivity as powerful tools for investigating the spectral signatures of connectivity disturbances in psychopathology.

Supplementary Material

Refer to Web version on PubMed Central for supplementary material.

Acknowledgments

The authors wish to acknowledge Nancy Hall-Brooks, Laurie Scott, Dr. Madeline Alexander, and David Crowley for their contribution to diagnostic screening of participants in the current study, along with Franziska Goer, Ashleigh Rutherford, and Rachel Clegg, for their assistance with participant recruitment and data collection.

Role of Funding Source: This research was supported by National Institute of Mental Health grants R01 MH068376 awarded to Dr. Pizzagalli and The William Rosenberg Family Foundation (Carol Silverstein and Jill Gotlieb); as well as R01 MH095809 and R01 MH101521 awarded to Dr. Pizzagalli. Dr. Whitton was partially supported by Fellowships from the Andrew P. Merrill Memorial Fund, the Brain and Behavior Research Foundation, and the National Health and Medical Research Council of Australia. The content is solely the responsibility of the authors and does not necessarily represent the official views of the National Institutes of Health.

References

1. Sheline YI, Price JL, Yan Z, Mintun MA. Resting-state functional MRI in depression unmasks increased connectivity between networks via the dorsal nexus. Proc Natl Acad Sci USA. 2010; 107:11020–11025. [PubMed: 20534464]
2. Veer IM, Beckmann C, Van Tol M-J, Ferrarini L, Milles J, Veltman D, et al. Whole brain resting-state analysis reveals decreased functional connectivity in major depression. Front Syst Neurosci. 2010; 4:1–10. [PubMed: 20204156]
3. Greicius MD, Flores BH, Menon V, Glover GH, Solvason HB, Kenna H, et al. Resting-state functional connectivity in major depression: abnormally increased contributions from subgenual cingulate cortex and thalamus. Biol Psychiatry. 2007; 62:429–437. [PubMed: 17210143]

4. Kaiser RH, Andrews-Hanna JR, Wager TD, Pizzagalli DA. Large-scale network dysfunction in major depressive disorder: a meta-analysis of resting-state functional connectivity. JAMA psychiatry. 2015; 72:603–611. [PubMed: 25785575]
5. Mantini D, Perrucci MG, Del Gratta C, Romani GL, Corbetta M. Electrophysiological signatures of resting state networks in the human brain. Proc Natl Acad Sci USA. 2007; 104:13170–13175. [PubMed: 17670949]
6. Chang C, Liu Z, Chen MC, Liu X, Duyn JH. EEG correlates of time-varying BOLD functional connectivity. Neuroimage. 2013; 72:227–236. [PubMed: 23376790]
7. O'Neill GC, Barratt EL, Hunt BA, Tewarie PK, Brookes MJ. Measuring electrophysiological connectivity by power envelope correlation: a technical review on MEG methods. Phys Med Biol. 2015; 60:R271–R295. [PubMed: 26447925]
8. Biswal B, Yetkin FZ, Haughton VM, Hyde JS. Functional connectivity in the motor cortex of resting human brain using echo-planar MRI. Magn Reson Med. 1995; 34:537–541. [PubMed: 8524021]
9. Greicius MD, Krasnow B, Reiss AL, Menon V. Functional connectivity in the resting brain: A network analysis of the default mode hypothesis. Proc Natl Acad Sci USA. 2003; 100:253–258. [PubMed: 12506194]
10. Raichle ME, MacLeod AM, Snyder AZ, Powers WJ, Gusnard DA, Shulman GL. A default mode of brain function. Proc Natl Acad Sci USA. 2001; 98:676–682. [PubMed: 11209064]
11. Andrews-Hanna JR, Reidler JS, Sepulcre J, Poulin R, Buckner RL. Functional-anatomic fractionation of the brain's default network. Neuron. 2010; 65:550–562. [PubMed: 20188659]
12. Dosenbach NUF, Fair DA, Cohen AL, Schlaggar BL, Petersen SE. A dual-networks architecture of top-down control. Trends Cogn Sci. 2008; 12:99–105. [PubMed: 18262825]
13. Chen AC, Oathes DJ, Chang C, Bradley T, Zhou Z-W, Williams LM, et al. Causal interactions between fronto-parietal central executive and default-mode networks in humans. Proc Natl Acad Sci USA. 2013; 110:19944–19949. [PubMed: 24248372]
14. Sheline YI, Barch DM, Price JL, Rundle MM, Vaishnavi SN, Snyder AZ, et al. The default mode network and self-referential processes in depression. Proc Natl Acad Sci USA. 2009; 106:1942–1947. [PubMed: 19171889]
15. Snyder HR. Major depressive disorder is associated with broad impairments on neuropsychological measures of executive function: A meta-analysis and review. Psychol Bull. 2013; 139:81–132. [PubMed: 22642228]
16. Kaiser RH, Andrews-Hanna JR, Spielberg JM, Warren SL, Sutton BP, Miller GA, et al. Distracted and down: neural mechanisms of affective interference in subclinical depression. Soc Cogn Affect Neurosci. 2015; 10:654–663. [PubMed: 25062838]
17. Pascual-Marqui RD, Lehmann D, Koukkou M, Kochi K, Anderer P, Saletu B, et al. Assessing interactions in the brain with exact low-resolution electromagnetic tomography. Philos Trans R Soc A. 2011; 369:3768–3784.
18. Canuet L, Tellado I, Couceiro V, Fraile C, Fernandez-Novoa L, Ishii R, et al. Resting-state network disruption and APOE genotype in Alzheimer's disease: a lagged functional connectivity study. PLoS One. 2012; 7:e46289. [PubMed: 23050006]
19. Hata M, Kazui H, Tanaka T, Ishii R, Canuet L, Pascual-Marqui RD, et al. Functional connectivity assessed by resting state EEG correlates with cognitive decline of Alzheimer's disease–An eLORETA study. Clin Neurophysiol. 2016; 127:1269–1278. [PubMed: 26541308]
20. Canuet L, Ishii R, Pascual-Marqui RD, Iwase M, Kurimoto R, Aoki Y, et al. Resting-state EEG source localization and functional connectivity in schizophrenia-like psychosis of epilepsy. PloS One. 2011; 6:e27863. [PubMed: 22125634]
21. Di Lorenzo G, Daverio A, Ferrentino F, Santarnecchi E, Ciabattini F, Monaco L, et al. Altered resting-state EEG source functional connectivity in schizophrenia: the effect of illness duration. Front Hum Neurosci. 2015; 9:234–245. [PubMed: 25999835]
22. Umesh DS, Tikka SK, Goyal N, Nizamie SH, Sinha VK. Resting state theta band source distribution and functional connectivity in remitted schizophrenia. Neurosci Lett. 2016; 630:199–202. [PubMed: 27484634]

23. Olbrich S, Olbrich H, Adamaszek M, Jahn I, Hegerl U, Stengler K. Altered EEG lagged coherence during rest in obsessive–compulsive disorder. Clin Neurophysiol. 2013; 124:2421–2430. [PubMed: 23968842]
24. Imperatori C, Farina B, Quintiliani MI, Onofri A, Gattinara PC, Lepore M, et al. Aberrant EEG functional connectivity and EEG power spectra in resting state post-traumatic stress disorder: A sLORETA study. Biol Psychol. 2014; 102:10–17. [PubMed: 25046862]
25. Imperatori C, Fabbricatore M, Innamorati M, Farina B, Quintiliani MI, Lamis DA, et al. Modification of EEG functional connectivity and EEG power spectra in overweight and obese patients with food addiction: An eLORETA study. Brain Imaging Behav. 2015; 9:703–716. [PubMed: 25332109]
26. Olbrich S, Tränkner A, Chittka T, Hegerl U, Schönknecht P. Functional connectivity in major depression: increased phase synchronization between frontal cortical EEG-source estimates. Psychiatry Res Neuroimaging. 2014; 222:91–99. [PubMed: 24674895]
27. Beck, AT., Steer, RA., Brown, GK. Beck Depression Inventory Manual. 2. San Antonio: The Psychological Corporation; 1996.
28. First, MB., Spitzer, RL., Gibbon, M., Williams, JB. Structured clinical interview for DSM-IV-TR Axis I disorders, research version, patient edition (SCID-I/P). New York: Biometric Research, New York State Psychiatric Institute; 2002.
29. Watson D, Weber K, Assenheimer JS, Clark LA, Strauss ME, McCormick RA. Testing a tripartite model: I. Evaluating the convergent and discriminant validity of anxiety and depression symptom scales. J Abnorm Psychol. 1995; 104:3–14. [PubMed: 7897050]
30. Pizzagalli DA, Peccoralo LA, Davidson RJ, Cohen JD. Resting anterior cingulate activity and abnormal responses to errors in subjects with elevated depressive symptoms: A 128-channel EEG study. Hum Brain Mapp. 2006; 27:185–201. [PubMed: 16035102]
31. Makeig S, Bell AJ, Jung T-P, Sejnowski TJ. Independent component analysis of electroencephalographic data. Adv Neural Inf Process Sys. 1996; 8:145–151.
32. Castellanos NP, Makarov VA. Recovering EEG brain signals: Artifact suppression with wavelet enhanced independent component analysis. J Neurosci Methods. 2006; 158:300–312. [PubMed: 16828877]
33. Perrin F, Pernier J, Bertnard O, Giard MH, Echallier JF. Mapping of scalp potentials by surface spline interpolation. Electroencephalogr Clin Neurophysiol. 1987; 66:75–81. [PubMed: 2431869]
34. Yeo BT, Krienen FM, Sepulcre J, Sabuncu MR, Lashkari D, Hollinshead M, et al. The organization of the human cerebral cortex estimated by intrinsic functional connectivity. J Neurophysiol. 2011; 106:1125–1165. [PubMed: 21653723]
35. Fuchs M, Kastner J, Wagner M, Hawes S, Ebersole JS. A standardized boundary element method volume conductor model. Clin Neurophysiol. 2002; 113:702–712. [PubMed: 11976050]
36. Mazziotta J, Toga A, Evans A, Fox P, Lancaster J, Zilles K, et al. A probabilistic atlas and reference system for the human brain: International Consortium for Brain Mapping (ICBM). Philos Trans R Soc Lond B Biol Sci. 2001; 356:1293–1322. [PubMed: 11545704]
37. Worrell GA, Lagerlund TD, Sharbrough FW, Brinkmann BH, Busacker NE, Cicora KM, O'Brien TJ. Localization of the epileptic focus by low-resolution electromagnetic tomography in patients with a lesion demonstrated by MRI. Brain Topogr. 2000; 12:273–282. [PubMed: 10912735]
38. Vitacco D, Brandeis D, Pascual-Marqui R, Martin E. Correspondence of event-related potential tomography and functional magnetic resonance imaging during language processing. Hum Brain Mapp. 2002; 17:4–12. [PubMed: 12203683]
39. Mulert C, Jager L, Schmitt R, Bussfeld P, Pogarell O, Moller HJ, et al. Integration of fMRI and simultaneous EEG: towards a comprehensive understanding of localization and time-course of brain activity in target detection. Neuroimage. 2004; 22:83–94. [PubMed: 15109999]
40. Dierks T, Jelic V, Pascual-Marqui RD, Wahlund LO, Julin P, Linden DEJ, et al. Spatial pattern of cerebral glucose metabolism (PET) correlates with localization of intracerebral EEG-generators in Alzheimer's disease. Clin Neurophysiol. 2000; 111:1817–1824. [PubMed: 11018498]
41. Pizzagalli DA, Oakes TR, Fox AS, Chung MK, Larson CL, Abercrombie HC, et al. Functional but not structural subgenual prefrontal cortex abnormalities in melancholia. Mol Psychiatry. 2003; 9:393–405.

42. Mobascher A, Brinkmeyer J, Warbrick T, Musso F, Wittsack HJ, Stoermer R, et al. Fluctuations in electrodermal activity reveal variations in single trial brain responses to painful laser stimuli - A fMRI/EEG study. Neuroimage. 2009; 44:1081–1092. [PubMed: 18848631]
43. Olbrich S, Mulert C, Karch S, Trenner M, Leicht G, Pogarell O, Hegerl U. EEG-vigilance and BOLD effect during simultaneous EEG/fMRI measurement. Neuroimage. 2009; 45:319–332. [PubMed: 19110062]
44. Zumsteg D, Friedman A, Wennberg RA, Wieser HG. Source localization of mesial temporal interictal epileptiform discharges: correlation with intracranial foramen ovale electrode recordings. Clin Neurophysiol. 2005; 116:2810–2818. [PubMed: 16253551]
45. Herrmann W, Fichte K, Freund G. Reflections on the topics: EEG frequency bands and regulation of vigilance. Pharmacopsychiatry. 1979; 12:237–245.
46. Dumlu K, Orhon Z, Özerdem A, Tural Ü, Ulaş H, Tunca Z. Treatment-induced manic switch in the course of unipolar depression can predict bipolarity: cluster analysis based evidence. J Affect Disord. 2011; 134:91–101. [PubMed: 21742381]
47. Ward AM, Schultz AP, Huijbers W, Dijk KR, Hedden T, Sperling RA. The parahippocampal gyrus links the default-mode cortical network with the medial temporal lobe memory system. Hum Brain Mapp. 2014; 35:1061–1073. [PubMed: 23404748]
48. Renner F, Siep N, Arntz A, van de Ven V, Peeters FPML, Quaedflieg CWEM, Huibers MJH. Negative mood-induction modulates default mode network resting-state functional connectivity in chronic depression. J Affect Disord. 2017; 208:590–596. [PubMed: 27810271]
49. Zamoscik V, Huffziger S, Ebner-Priemer U, Kuehner C, Kirsch P. Increased involvement of the parahippocampal gyri in a sad mood predicts future depressive symptoms. Soc Cog Affect Neurosci. 2014; 9:2034–2040.
50. Ma C, Ding J, Li J, Guo W, Long Z, Liu F, et al. Resting-state functional connectivity bias of middle temporal gyrus and caudate with altered gray matter volume in major depression. PLoS One. 2012; 7:e45263. [PubMed: 23028892]
51. Northoff G. How do resting state changes in depression translate into psychopathological symptoms? From 'Spatiotemporal correspondence'to 'Spatiotemporal Psychopathology'. Curr Opin Psychiatry. 2016; 29:18–24. [PubMed: 26651006]
52. Engel AK, Fries P. Beta-band oscillations—signalling the status quo? Curr Opin Neurobiol. 2010; 20:156–165. [PubMed: 20359884]
53. Engel AK, Fries P, Singer W. Dynamic predictions: oscillations and synchrony in top–down processing. Nat Rev Neurosci. 2001; 2:704–716. [PubMed: 11584308]
54. Kühn AA, Williams D, Kupsch A, Limousin P, Hariz M, Schneider GH, et al. Event-related beta desynchronization in human subthalamic nucleus correlates with motor performance. Brain. 2004; 127:735–746. [PubMed: 14960502]
55. Weinberger M, Mahant N, Hutchison WD, Lozano AM, Moro E, Hodaie M, et al. Beta oscillatory activity in the subthalamic nucleus and its relation to dopaminergic response in Parkinson's disease. J Neurophysiol. 2006; 96:3248–3256. [PubMed: 17005611]
56. Toledo JB, López-Azcárate J, Garcia-Garcia D, Guridi J, Valencia M, Artieda J, et al. High beta activity in the subthalamic nucleus and freezing of gait in Parkinson's disease. Neurobiol Dis. 2014; 64:60–65. [PubMed: 24361601]
57. Chen CC, Litvak V, Gilbertson T, Kühn A, Lu CS, Lee ST, et al. Excessive synchronization of basal ganglia neurons at 20 Hz slows movement in Parkinson's disease. Exp Neurol. 2007; 205:214–221. [PubMed: 17335810]
58. Pfurtscheller G, Stancak A, Neuper C. Post-movement beta synchronization. A correlate of an idling motor area? Electroencephalogr Clin Neurophysiol. 1996; 98:281–293. [PubMed: 8641150]
59. Pesaran B, Nelson MJ, Andersen RA. Free choice activates a decision circuit between frontal and parietal cortex. Nature. 2008; 453:406–409. [PubMed: 18418380]
60. Buschman TJ, Miller EK. Top-down versus bottom-up control of attention in the prefrontal and posterior parietal cortices. Science. 2007; 315:1860–1862. [PubMed: 17395832]
61. Laufs H, Krakow K, Sterzer P, Eger E, Beyerle A, Salek-Haddadi A, Kleinschmidt A. Electroencephalographic signatures of attentional and cognitive default modes in spontaneous

brain activity fluctuations at rest. Proc Natl Acad Sci USA. 2003; 100:11053–11058. [PubMed: 12958209]

62. Hlinka J, Alexakis C, Diukova A, Liddle PF, Auer DP. Slow EEG pattern predicts reduced intrinsic functional connectivity in the default mode network: an inter-subject analysis. Neuroimage. 2010; 53:239–246. [PubMed: 20538065]
63. Neuner I, Arrubla J, Werner CJ, Hitz K, Boers F, Kawohl W, Shah NJ. The default mode network and EEG regional spectral power: a simultaneous fMRI-EEG study. PLoS One. 2014; 9:e88214. [PubMed: 24505434]
64. Calhoun VD, Miller R, Pearlson G, Adalı T. The chronnectome: time-varying connectivity networks as the next frontier in fMRI data discovery. Neuron. 2014; 84:262–274. [PubMed: 25374354]
65. Kaiser RH, Whitfield-Gabrieli S, Dillon DG, Goer F, Beltzer M, Minkel J, et al. Dynamic resting-state functional connectivity in major depression. Neuropsychopharmacology. 2015; 41:1822–1830. [PubMed: 26632990]
66. Buzsáki G, Draguhn A. Neuronal oscillations in cortical networks. Science. 2004; 304:1926–1929. [PubMed: 15218136]
67. Liu Q, Farahibozorg S, Porcaro C, Wenderoth N, Mantini D. Detecting large-scale networks in the human brain using high-density electroencephalography. 2016:077107. bioRxiv.
68. Cho J-H, Vorwerk J, Wolters CH, Knösche TR. Influence of the head model on EEG and MEG source connectivity analyses. Neuroimage. 2015; 110:60–77. [PubMed: 25638756]

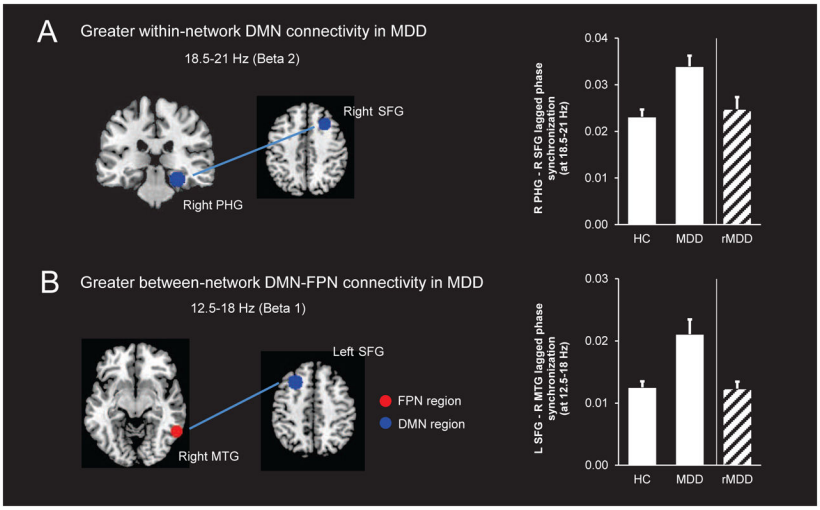

Figure 1.

Relative to the HC group, the MDD group showed significantly greater within-network lagged phase synchronization in the DMN at the beta 2 frequency band (p<0.05 FWE), specifically between the right parahippocampal gyrus (PHG) and right superior frontal gyrus (SFG) (**A**). The MDD group also showed significantly greater between-network lagged phase synchronization between the DMN and FPN at the beta 1 frequency band compared to HCs (p<0.001 uncorrected), specifically between the left SFG (a DMN region) and the right middle temporal gyrus (MTG; a FPN region) (**B**). Follow-up one-way ANOVAs showed that both indices of connectivity were lower in those with rMDD relative to the MDD group, and the rMDD and HC groups did not differ. For the purposes of visualization, ROIs shown here are displayed on a 2×2×2 MNI template brain (5 mm resolution is used in eLORETA for analyses).

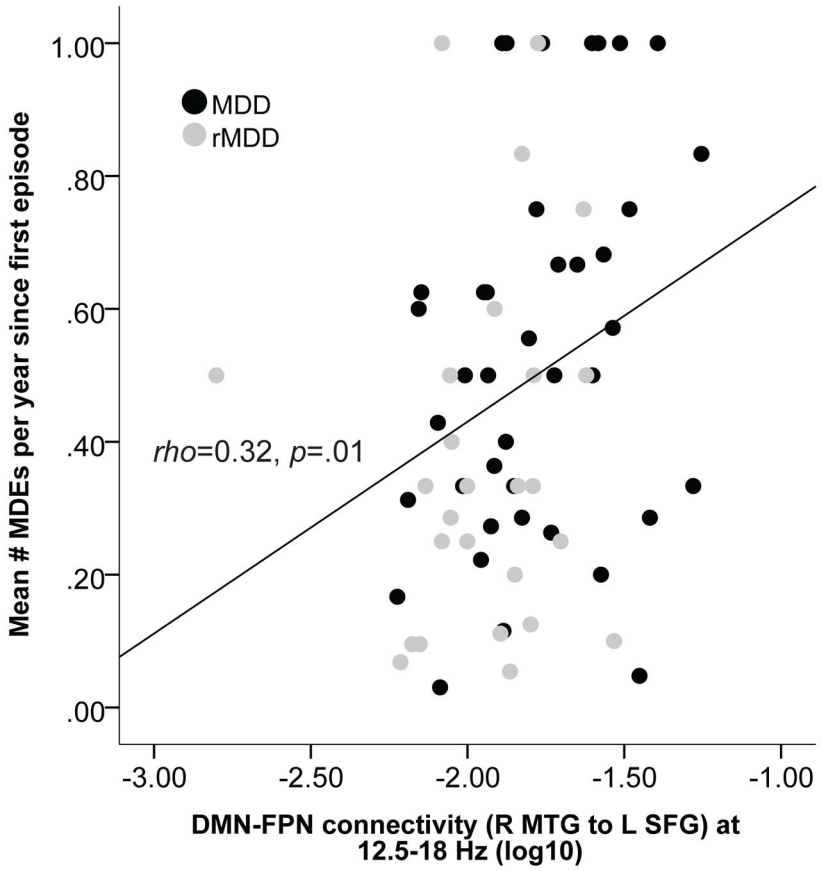

Figure 2.

Scatterplot showing the Spearman's rank order correlation between disease severity (operationalized as the mean number of major depressive episodes per year since first depression onset) and the strength of between-network DMN-FPN connectivity (12.5 – 18 Hz) in the MDD and rMDD groups.

Table 1

Seed coordinates from the DMN and FPN

Network	x	y	x	Anatomical structure
Default Mode Network (DMN)				
L DMN-A	−27	23	48	superior frontal gyrus
R DMN-A	27	23	48	superior frontal gyrus
L DMN-B	−41	−60	29	angular gyrus
R DMN-B	41	−60	29	angular gyrus
L DMN-C	−64	−20	−9	middle temporal gyrus
R DMN-C	64	−20	−9	middle temporal gyrus
Mid DMN-D	0	49	18	medial frontal gyrus
L DMN-E	−25	−32	−18	parahippocampal gyrus
R DMN-E	25	−32	−18	parahippocampal gyrus
Mid DMN-F	0	−52	26	posterior cingulate
Fronto-Parietal Network (FPN)				
L FPN-A	−40	50	7	frontal pole
R FPN-A	40	50	7	frontal pole
L FPN-B	−43	−50	46	supramarginal gyrus
R FPN-B	43	−50	46	supramarginal gyrus
L FPN-C	−57	−54	−9	middle temporal gyrus
R FPN-C	57	−54	−9	middle temporal gyrus
Mid FPN-D	0	22	47	paracingulate gyrus
Mid FPN-E	0	4	29	cingulate gyrus
Mid FPN-F	0	−76	45	precuneus cortex

Note. Coordinates are in MNI space. DMN=Default Mode Network; FPN=Fronto-Parietal Network; L=Left hemisphere seed; R=Right hemisphere seed; Mid=Midline seed. Labels should be considered approximate because of the uncertain boundaries of the areas and activation patterns.

Biol Psychiatry Cogn Neurosci Neuroimaging. Author manuscript; available in PMC 2019 January 01.

Table 2

Demographic and clinical characteristics

	HC (*n*=79)	MDD (*n*=65)	rMDD (*n*=30)	test value	*df*	*p* value
Demographics						
Female, *N* (%)	58 (73.4)	52 (80.0)	22 (73.3)	X^2=0.97	2	.62
Age in years	27.5 (8.2)^a	29.1 (8.4)^{a,b}	32.7 (14.6)^b	*F*=3.25	171	.04
Years of education	16.5 (2.5)	16.0 (2.5)	16.5 (2.2)	*F*=0.91	171	.41
Caucasian, *N* (%)	60 (75.9)	41 (63.1)	22 (73.3)	X^2=2.97	2	.23
Clinical characteristics						
Number of MDEs	-	4.1 (4.0)	2.4 (1.5)	*t*=2.16	68	.03
Age of first MDE	-	19.1 (8.8)	22.2 (12.6)	*t*=1.19	68	.24
Mean episodes per year since first MDE	-	0.6 (0.5)	0.4 (0.4)	*t*=1.70	68	.09
Lifetime comorbidities, *N* (%)	-	37 (56.9)	8 (26.7)	X^2=7.54	1	.006
Current comorbidities, *N* (%)	-	23 (35.4)	-	-	-	-
Current psychotropic medications, *N* (%)	-	10 (15.9)	-	-	-	-
Symptomatology						
BDI-II	0.7 (1.6)^a	26.6 (9.9)^b	2.8 (3.4)^a	*F*=331.41	171	<.001
MASQ GDD	13.7 (3.3)^a	37.3 (10.1)^b	17.6 (6.1)^c	*F*=213.60	171	<.001
MASQ AD	44.3 (10.9)^a	82.9 (11.2)^b	48.6 (12.4)^a	*F*=223.71	171	<.001
MASQ GDA	12.8 (2.1)^a	25.0 (8.3)^b	14.8 (3.7)^a	*F*=93.58	171	<.001
MASQ AA	17.7 (1.2)^a	27.7 (9.7)^b	19.0 (2.9)^a	*F*=51.20	171	<.001

Note.

^{a,b,c}Means in a row without a common superscript letter differ as analyzed by one-way ANOVA (p<0.05); table values are in the format Mean (Std. Dev) unless otherwise noted.